JTTEE5 15:689-694
DOI: 10.1361/105996306X146749
1059-9630/$19.00 © ASM International

Microstructure and Abrasion Resistance of Plasma Sprayed Titania Coatings

P. Ctibor, K. Neufuss, and P. Chraska

(Submitted February 20, 2006; in revised form June 9, 2006)

Agglomerated titania nanopowder and a "classical" titania were sprayed by the high throughput water-stabilized plasma (WSP) and thoroughly compared. Optical microscopy with image analysis as well as mercury intrusion porosimetry were used for quantification of porosity. Results indicate that the "nano" coatings in general exhibit finer pores than coatings of the "conventional" micron-sized powders. Mechanical properties such as Vickers microhardness and slurry abrasion response were measured and linked to the structural investigation. Impact of the variation in the slurry composition on wear resistance of tested coatings and on character of the wear damage is discussed. The overall results, however, suggest that the "nano" coatings properties are better only for carefully selected sets of spraying parameters, which seem to have a very important impact.

Keywords image analysis, slurry abrasion, titanium oxide, water-stabilized plasma

1. Introduction

Titania itself is not a material with excellent mechanical properties for heavy-duty engineering spray applications (Ref 1). Its main role for many years was to serve as an admixture to other spray materials. The most famous case of this is the "AT" family of materials based on alumina and titania. Erosion, abrasion, and flexure strength (Ref 2) and also adhesion after thermal cycling (Ref 3) increases for AT compared with pure alumina. During the last 10 to 15 years other uses of titania in a composite can be found:

- Titania is a base or a component of various biocompatible materials (Ref 4-6).
- Titania is a load-bearing component in composites with plastics such as polyacrylates (Ref 7, 8).
- Cermets with titania are reported occasionally (Ref 9).

Study of mechanical properties of titania itself started to be of interest in the context of the photocatalytic effect of titania and in connection with development of titania nanomaterials and its commercialization as "nanostructured thermal spray grade powders" (TSGP). However, greater attention is still paid to alumina-titania nanocoatings (Ref 10, 11). Some results dealing with the nanopowder-based pure titania coatings using air plasma spraying (APS) are available (Ref 12-16), but not all the processing and technological variables affecting the properties of the final coating are well understood.

Microhardness values given in the literature for TiO_2 thermally sprayed coatings are mostly in the range 7 to 9 GPa for $HV_{0.3}$ (Ref 1). With lower loads, local hardness differences were observed, and low values were found in areas with low O/Ti ratios. The Young's modulus *E* of the sintered rutile form of titania is 282 GPa. A Young's modulus of 164 GPa was found for a coating produced using the high-velocity oxyfuel (HVOF) process. For HVOF coatings, the results obtained using different measurement methods were identical; for APS coatings, on the other hand, results varied widely. In another study, APS coatings showed no scatter in results for different methods, but a lower value of Young's modulus was obtained. For the HVOF coating (Ref 1), the value can be estimated to be approximately 140 GPa. Other values reported for APS coatings are in the range 88 to 134 GPa. Poisson's ratio is given as 0.33 for an APS coating and 0.25 for a coating produced by the HVOF process (Ref 1).

In comparison to other oxide coatings, APS sprayed titanium oxide coatings are generally characterized by an intermediate but satisfactory wear resistance, which has led to their application in mechanical engineering (light bearings, pump seals, etc.). The abrasion wear resistance of APS pure titania coatings is similar to the group of AT coatings. A similar result is found if the abrasion wear resistance of HVOF coatings is compared with detonation gun (DGS) coatings. Also, a relatively high erosion wear resistance is reported. A decrease in hardness and abrasion wear resistance is reported to be connected to a strong increase in oxygen deficiency (Ref 1).

The titania coatings made of the "conventional" feedstock powders exhibit microhardness around 8 to 8.5 GPa (Ref 12, 16), but slightly higher values can be expected for coatings made of nanopowder as the feedstock. All the available literature data were obtained using commercial gas stabilized APS, HVOF, or DGS systems. The aim of this work was to spray various available titania-based nanopowders using the high-throughput water-stabilized plasma system (WSP).

This article was originally published in *Building on 100 Years of Success, Proceedings of the 2006 International Thermal Spray Conference* (Seattle, WA), May 15-18, 2006, B.R. Marple, M.M. Hyland, Y.-Ch. Lau, R.S. Lima, and J. Voyer, Ed., ASM International, Materials Park, OH, 2006.

P. Ctibor, K. Neufuss, and **P. Chraska,** Institute of Plasma Physics ASCR, Za Slovankou 3, 182 00 Praha 8, Czech Republic. Contact e-mail: ctibor@ipp.cas.cz.

2. Experimental

2.1 Feedstocks and Coating Production

Altium TiNano 40 VHP (Ti NanoCoat VHP TSGP, Altair Nanomaterials Inc., Reno, NV) is a nanosized titanium dioxide product. Thermal spray grade powder (TSGP) was prepared from nanometric powder by its agglomeration (agglomerated nanopowder AN). The fraction from 45 to 75 μm in size was used for spray experiments at various processing conditions. For comparison, a "conventional" powder—crushed and sieved natural rutile form of TiO_2 (NR) with a particle size for spraying between 63 and 125 μm—was also used. Optimization of spray setup parameters was carried out before spraying of experimental AN coatings. In the case of NR coating for majority of tests, only feeding distance $FD = 45$ mm and spray distance $SD = 350$ mm were used.

Samples were produced using the high-throughput water-stabilized plasma spray system WSP 500 (Institute of Plasma Physics, Prague, Czech Republic). This system operates at 160 kW arc power and can process up to several tens of kilograms of the spray material per hour. The spray parameters varied in the experiments are denoted as follows: *FD* is the feeding distance (i.e., distance from the spray gun nozzle to the tip of the feeding injector); *SD* denotes the spray distance (i.e., distance from the spray gun nozzle to the substrate). Identification of a sample then consists of an acronym for the material and *FD*-*SD* (for instance AN 52-450 means nanopowder sprayed at $FD = 52$ mm and $SD = 450$ mm). The powder was fed in by compressed air through two injectors, and thickness of the produced coatings was about 1.5 mm. Stainless steel coupons were used as substrates. Some of the coatings were then stripped off for characterizations such as intrusion porosimetry and for annealing.

2.2 Annealing

Annealing of as-sprayed deposits was carried out in a laboratory furnace at a temperature of 1250 °C for 1 h. Heating as well as cooling was done in air at a rate of 7 K/min in both cases. The annealing temperature was selected with respect to sintering temperature, which is usually considered to be 0.7 of the melting point (T_m of titania is 1870 °C). The temperature used lies well above the anatase/rutile phase transformation and is high enough to change the microstructure significantly.

3. Characterization Techniques

3.1 Porosity Investigation by Image Analysis

Porosity was studied by optical microscopy on polished cross sections. Micrographs were taken with a CCD camera and processed using image analysis (IA) software (Lucia G, Laboratory Imaging, Czech Republic). A minimum of ten images of microstructures, taken from various areas of a cross section for each sample, were analyzed. The magnification used was 250× in all cases, allowing all objects with size of 3 μm or more to be included in the analysis.

For a better description of the porosity certain additional criteria were introduced:

- *NV* denotes the number of voids per unit area of the cross section.
- "Equivalent diameter" (*ED*) of voids represents their size distribution and the "Maximal *ED*" (ED_{max}) the size of the largest void detected (approximation in two-dimensional projection).
- "Circularity" (*CI*) describes the shape of pores where "1" represents a perfect circle and "0" a linear void projection; it is calculated for at least ten images. "Minimal *CI*" (CI_{min}) is then a parameter used for distinction between samples; small CI_{min} indicates rather a lamellar coating structure while high CI_{min} suggests a "sintered-like" structure.

It is important to note that the resolution of the techniques used in this work is sufficient to provide information about interlamellar pores, but not about the fine vertical cracks that are common in the plasma sprayed coatings.

3.2 Mercury Intrusion Porosimetry

For detection of the smallest voids and recording of size distribution of voids over a wide range, mercury intrusion porosimetry (MIP; Auto Pore III, Micromeritics, Norcross, GA) has been used for several samples representing distinct states of the microstructure. Common assumptions of constant contact angle and constant surface tension during the measurement as well as globular shape of pores were used. Accuracy of the pore diameter determination was about ±0.5%.

3.3 Microhardness Measurement

Microhardness was measured by the Hanemann microhardness head (C. Zeiss, Jena, Germany) mounted on an optical microscope with a fixed load of 1 N and a Vickers indenter. Twenty indentations from various areas of a cross section for each sample were analyzed.

3.4 Slurry Abrasion Response (SAR) Tests

Slurry abrasion response of coatings (SAR test) was measured according to ASTM standard G 75-95 (Ref 17). The applied force was 22.24 N per specimen. The test was run for 4 h in 2 h increments with mass loss being measured at the end of each 2 h increment, when the specimens were ultrasonically cleaned and weighed. The wear loss is expressed in grams per square centimeter of the sample surface. Accuracy of the measurement is about ±5%.

Two different sizes of white alumina abrasive powder were used. The first series of tests was made with fine powder (40 to 50 μm) and second series with coarse powder (850 μm to 1 mm); water was used in both cases as the fluid medium. The main reason for the selected sizes was the fact that the fine powder particles are smaller than the splat size of the coating, whereas the coarse powder particles are significantly larger than the splats.

4. Results and Discussion

4.1 Microstructure—General Remarks

First of all, it is interesting and necessary to note that despite substantially higher plasma jet temperatures of the

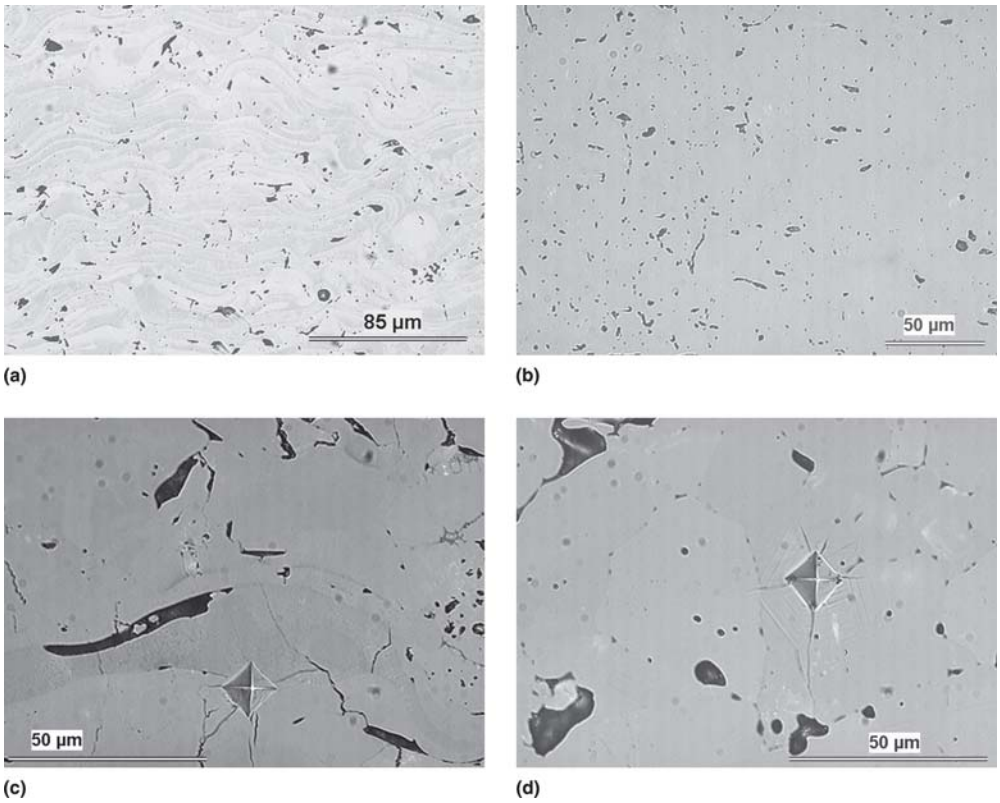

Fig. 1 Optical micrograph of the cross section of (a) agglomerated nanopowder (AN) coating FD52-SD350, (b) annealed coating AN-FD52-SD350, (c) natural rutile (NR) coating with Vickers indent, and (d) annealed NR coating with indent

WSP, and subsequently a higher melting power than those of commercial gas-stabilized systems on the market, distinct features of nanostructure were preserved in coatings, due to careful selection of the processing parameters. If it were not so, spraying of nanopowders with WSP would not be substantiated.

4.2 Image Analysis (IA)

Figure 1 shows examples of typical microstructures evaluated. Figures 2 to 5 show histograms of various data for different spraying parameters and different materials in the as-sprayed and annealed conditions. Porosity (Fig. 2) as well as the number of voids per square millimeter *NV* (Fig. 3) exhibit a minimum for the as-sprayed deposit AN 52-350. The natural rutile (NR) coating has a similar low *NV*, but the total porosity of this coating is not correspondingly low. This finding might be explained by the presence of rather large-sized voids in NR. This is confirmed by results of measurement of the largest detected objects ED_{max} (Fig. 4)—ED_{max} of the NR coating is higher than ED_{max} of all AN coatings.

Figure 5 shows the highest CI_{min} equal to 0.18 for sample AN 52-350, suggesting that voids in this sample, even though far from circular (e.g., flat pores, cracks), are more convex than for any other processing parameters. Combining results of the porosity measurements, *NV*, ED_{max}, and CI_{min} suggests the sample 52-350 is the most homogeneous and isotropic in the section plane, assuming that all voids affecting CI_{min} value are intersplat

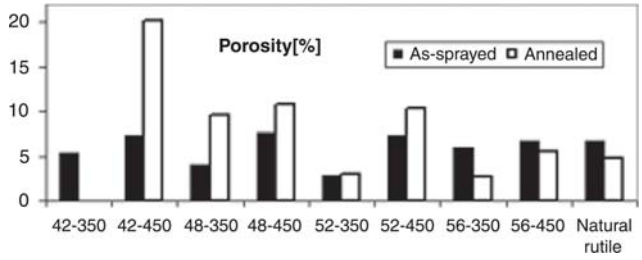

Fig. 2 Porosity of variety of AN coatings and one NR coating, data based on image analysis

flat pores oriented along the surface plane. In addition, pores larger than 10 µm are absent only in this coating AN 52-350 (Fig. 4). All these facts together suggest spraying with *FD* = 52 and *SD* = 350 as the best processing parameters for the given nanopowder.

However, in general for AN samples it can be concluded that the longer the *SD*, the higher the *NV*, and ED_{max}. This is probably due to partial solidification and a loss of velocity of particles before impact at long *SD*; particles do not have high enough velocity to flatten well. NR feedstock is larger than AN feedstock, and therefore the resulting porosity of NR coatings at similar spray parameters is larger, but seems to have lamellar character (large ED_{max} and small CI_{min}).

Results for *FD* = 56 mm suggest a high concentration of voids, which are quite fine and "globular." That indicates most

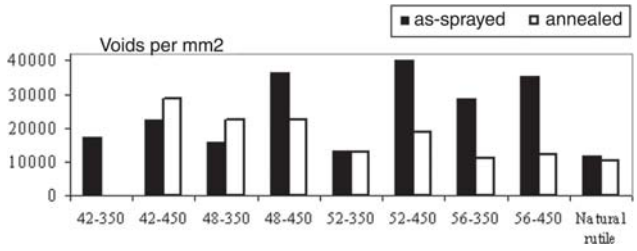

Fig. 3 Number of voids per mm^2 of variety of AN coatings and one NR coating, data based on image analysis

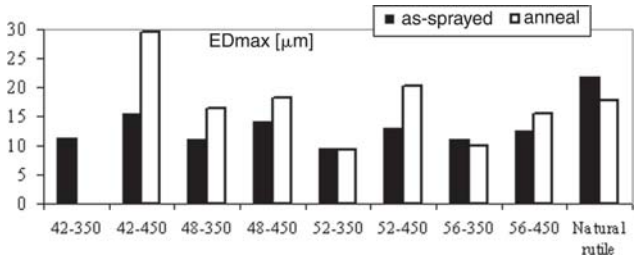

Fig. 4 Maximal equivalent diameter ED_{max} of variety of AN coatings and one NR coating, data based on image analysis

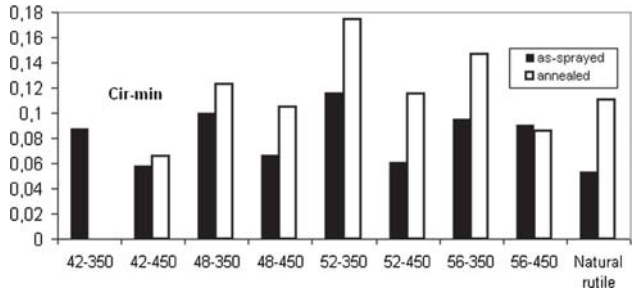

Fig. 5 Circularity minima of variety of AN coatings and one NR coating, data based on image analysis

probably poor melting compared with FD 52. Feeding distances under 50 mm result in a larger porosity suggesting that the injection of powder is not optimal, and feedstock particles do not properly penetrate the plasma jet. Agglomerated particles are less compact, on entry into the plasma jet they easily disintegrate, and each disintegrated part then follows its own trajectory, some of them at the edge of the plasma jet. Resulting structure in that case exhibits unmelted particles embedded in melted and partially melted ones, and consequently a large porosity is recorded.

Looking at the annealed samples, it is clear that for short *FD*s the annealing leads to an increase of porosity. Parameters of the as-sprayed "best" coating AN 52-350 are improved by annealing only slightly. The character of the NR coating also remains almost unchanged.

In contrast, marked changes of originally similar AN coatings 42-450 and 56-350 are seen. In the first case the porosity markedly increases after annealing, while in the second case it decreases. The reason for this behavior is likely to be found in

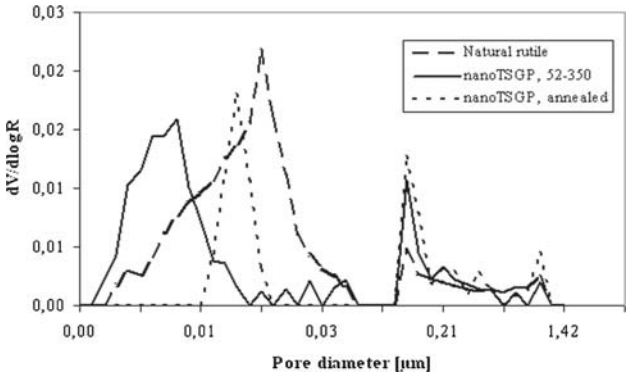

Fig. 6 Mercury intrusion porosimetry of as-sprayed AN, annealed AN, and as-sprayed NR coating

different dwell times of particular particles in the plasma jet of different temperatures during spraying.

4.3 Mercury Intrusion Porosimetry (MIP)

Mercury intrusion porosimetry results are shown in Fig. 6. It is interesting to note the shift in the maximum counts of pores: for NR it is at a larger pore diameter (~0.25 μm), while for AN as-sprayed coating it is at a lower value (~0.05 μm).

However, the interval of detected voids with a minimum around 0.02 μm is almost the same for both AN and NR coatings, while the maximum for annealed sample is rather close to that of NR and the interval of void sizes is narrow. The other interesting point is that the detected sizes split into two separate intervals: one below roughly 1.3 μm, the other one above approximately 2.5 μm. The small part is below the resolution limit of IA, and therefore only the larger voids were processed in the above results. The gap in the size distribution suggests a fundamental change in the void character, such as between cracks and pores, and so forth. However, further studies are needed in this respect.

4.4 Microhardness

Results of microhardness measurements are summarized in Fig. 7. The best value for the as-sprayed state is for sample AN 52-350. However, the apparent dependence of microhardness on *SD* for a given *FD* is not significant given the error bars. In general, slightly higher values of microhardness are recorded for larger *FD* (52 and 56 mm). Annealing improves the microhardness in all cases and to a similar extent.

4.5 Slurry Abrasion Response (SAR)

The results of SAR tests are presented in Fig. 8 and 9. The procedure used (ASTM standard G 75-95, Ref 17) works with the mass loss, while for porous coatings probably the volume loss would be better. However, as reported in Ref 18, the phase content and structural morphology of all tested samples are similar. The density, measured on similar but stripped-off samples, was in the interval from 4.04 g/cm^3 for AN 52-350 sample and 4.20 g/cm^3 for both NR samples up to 4.28 g/cm^3 for annealed AN coatings (Ref 18). The volume losses can be then calculated, and the general trends are similar to those of the mass loss. How-

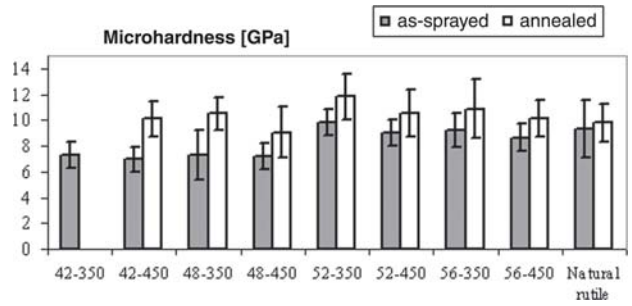

Fig. 7 Microhardness of variety of AN coatings and one NR coating, data based on $HVm_{0,1}$ test

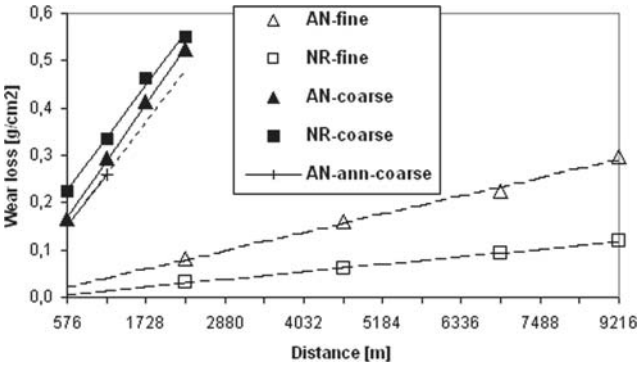

Fig. 8 Wear loss of AN, NR, and annealed agglomerated nanopowder (AN-ann) coating in fine and coarse powder as the slurry component

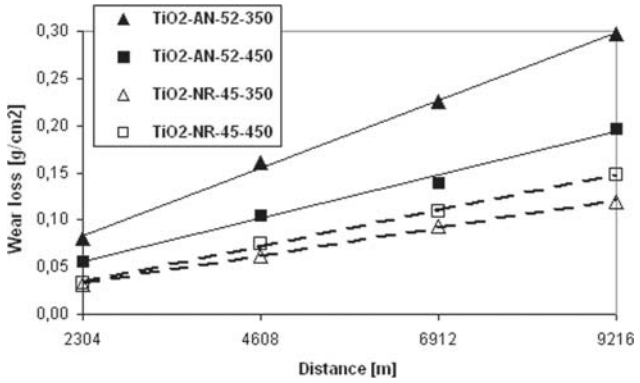

Fig. 9 Wear loss of AN and NR coatings with SD 350 and 450 mm in fine powder as the slurry component

ever, more important than the absolute values of the losses is the pattern of behavior:

- Two main differences between the fine and the coarse slurry can be clearly seen from Fig. 8: (a) wear losses for tests in the fine slurry are significantly lower than for the coarse slurry and (b) differences between various coatings are less distinct for the coarse slurry than for fine slurry.
- In the case of coarse slurry, the entire coating thickness of any type of coating is fully removed after a relatively short test distance (recalculated volume wear loss around 350 mm^3).
- Wear losses of NR coatings are less sensitive to SD than of AN coatings (Fig. 9).
- Both coatings from NR exhibit better slurry abrasion resistance compared with AN coatings.
- Annealing of AN samples does not seem to have any significant effect on the wear resistance.

The unexpected result that the agglomerated nanopowder-based coatings (AN) have lower abrasion resistance than the natural rutile-based coatings (NR) could be explained by two facts:

- Only one type of nano titania was chosen for testing, that is, the hardest one, as would be a logical choice for a conventional coating. However, as it has been pointed out by Jordan et al. for plasma sprayed nano alumina-titania coatings (Ref 10), the hardest nanocoating may not be the best one for wear resistance.
- Studied AN coatings were more brittle compared with NR coatings as observed during the sample preparation. The exact cause of that brittleness is still not fully understood, but it is likely connected to a higher state of the internal stress. Consequently, more cracks materialize as a way of the internal stress relaxation leading to a faster abrasion of the coating.

5. Conclusions

- Agglomerated nano titania powders AN can be sprayed even with the high enthalpy, high-throughput WSP, and certain distinct features of nanostructure are well formed in coatings.
- Microstructural investigation and porosity measurements of as-sprayed AN samples show that homogeneous coatings with a low porosity can be made by a careful selection of the processing parameters; coatings made from conventional titania powder (NR) are rather lamellar and due to larger feedstock size and wider particle size distribution are also less homogeneous.
- Variety of microstructural parameters proved that additional annealing of the as-sprayed coatings brings measurable structural and property improvements only for coatings produced with the feeding distance *FD* longer than 50 mm.
- Microhardness and SAR were measured for variety of processing parameters and compared. Dependence of microhardness on processing parameters (*SD* for a given *FD*) is not significant. In general, slightly higher values of microhardness are recorded for larger *FD*. Annealing improves the microhardness to a similar extent in all tested cases.
- Slurry abrasion resistance was better for NR than for AN powder; since only the hardest AN samples were tested this conclusion must be regarded as tentative and additional work is necessary on other AN samples.

Acknowledgment

The authors acknowledge general support of the Academy of Science of the Czech Republic under project AV0 Z 20430508.

Part of the experiments were supported from project CV 1Q5 200430560.

References

1. L.-M. Berger, Titanium Oxide—New Opportunities for an Established Coating Material, *Proceedings of the International Thermal Spray Conference 2003,* C. Berndt, Ed., CD-ROM section 024.pdf, DVS Verlag, Düsseldorf, 2003
2. R. Westergard, N. Axen, U. Wiklund, and S. Hogmark, An Evaluation of Plasma Sprayed Ceramic Coatings by Erosion, Abrasion and Bend Testing, *Wear,* 2000, **246**(1-2), p 12-19
3. M. Jakubov, P. Ctibor, and K. Neufuss, Thermal Fatigue Testing of Ceramic Coatings Produced by Water-Stabilized Plasma Gun, *Thermal Spray Connects: Explore Its Surfacing Potential* (Basel, Switzerland), May 2-4, 2005, C.C. Berndt, Ed., DVS, 2005, p 1183-1186
4. H. Li, K.A. Khor, and P. Cheang, Titanium Dioxide Reinforced Hydroxyapatite Coatings Deposited by High Velocity Oxy-Fuel (HVOF) Spray, *Biomaterials,* 2002, **23**(1), p 85-91
5. J. Li, S. Forberg, and L. Hermansson, Evaluation of the Mechanical Properties of Hot Isostatically Pressed Titania and Titania-Calcium Phosphate Composites, *Biomaterials,* 1991, **12**(4), p 438-440
6. M. Manso, S. Ogueta, P. García, J. Pérez-Rigueiro, C. Jiménez, J.M. Martínez-Duart, and M. Langlet, Mechanical and in vitro Testing of Aerosol-Gel Deposited Titania Coatings for Biocompatible Applications, *Biomaterials,* 2002, **23**(2), p 349-356
7. F.X. Perrin, V. Nguyen, and J.L. Vernet, Mechanical Properties of Polyacrylic-Titania Hybrids—Microhardness Studies, *Polym.,* 2002, **43**(23), p 6159-6167
8. S.H. Lee, C. Tekmen, and W.M. Sigmund, Three-Point Bending of Electrospun TiO_2 Nanofibers, *Mater. Sci. Eng. A,* 2005, **398**(1-2), p 77-81
9. J. Li, Y. Sun, X. Sun, and J. Qiao, Mechanical and Corrosion-Resistance Performance of Electrodeposited Titania-Nickel Nanocomposite Coatings, *Surf. Coat. Technol.,* 2005, **192**(2-3), p 331-335
10. E.H. Jordan, M. Gell, Y.H. Sohn, D. Goberman, L. Shaw, S. Jiang, M. Wang, T.D. Xiao, Y. Wang, and P. Strutt, Fabrication and Evaluation of Plasma Sprayed Nanostructured Alumina-Titania Coatings with Superior Properties, *Mater. Sci. Eng. A,* 2001, **301**(1), p 80-89
11. M. Gell, E.H. Jordan, Y.H. Sohn, D. Goberman, L. Shaw, and T.D. Xiao, Development and Implementation of Plasma Sprayed Nanostructured Ceramic Coatings, *Surf. Coat. Technol.,* 2001, **146-147,** p 48-54
12. A. Ibrahim, R.S. Lima, B.R. Marple, and C.C. Berndt, Fatigue and Mechanical Properties of Nanostructured vs Conventional Titania (TiO_2) Coatings, *Thermal Spray Connects: Explore Its Surfacing Potential,* May 2-4, 2005 (Basel, Switzerland), C.C. Berndt, Ed., DVS, 2005, p 855-859
13. R.S. Lima and B.R. Marple, Nanostructured and Conventional Titania Coatings for Abrasion and Slurry-Erosion Resistance Sprayed via APS, VPS and HVOF, *Thermal Spray Connects: Explore Its Surfacing Potential,* May 2-4, 2005 (Basel, Switzerland), C.C. Berndt, Ed., DVS, 2005, p 552-557
14. R.S. Lima and B.R. Marple, From APS to HVOF Spraying of Conventional and Nanostructured Titania Feedstock Powders: A Study on the Enhancement of the Mechanical Properties, *Surf. Coat. Technol.,* 2006, **200,** p 3428-3437
15. H. Du, H. Chen, B.K. Moom, J.H. Shin, and S.W. Lee, Effect of Plasma Spraying Condition on Deposition Efficiency, Microstructure and Microhardness of TiO_2 Coating, *Adv. Technol. Mater. Mater. Process.,* 2004, **6**(2), p 152-157
16. R.S. Lima and B.R. Marple, Near-Isotropic Air Plasma Sprayed Titania, *Acta Mater.,* 2004, **52**(5), p 1163-1170
17. "Test Method for Determination of Slurry Abrasivity (Miller Number) and Slurry Abrasion Response of Materials (SAR Number)," G 0075-01, *Annual Book of ASTM Standards,* Volume 03.02, Aug 2005
18. P. Ctibor, K. Neufuss, J. Dubsky, B. Kolman, P. Rohan, and P. Chraska, Spraying of Agglomerated TiO_2 Nanopowder by Water-Stabilized Plasma, *Building on 100 Years of Success,* May 15-18, 2006 (Seattle, WA), B.R. Marple et al., Ed., ASM, International, 2006, paper s9-11-11949